Molecular and Cellular Biochemistry (2018) 444:43–52
https://doi.org/10.1007/s11010-017-3229-0

# Mir-513a-3p contributes to the controlling of cellular migration processes in the A549 lung tumor cells by modulating integrin β-8 expression

**Marina Bonfogo da Silveira[1] · Kelvin Furtado Lima[2] · Andrea Renata da Silva[3] · Robson Augusto Souza dos Santos[4] · Karen C. M. Moraes[1]**

Received: 1 August 2017 / Accepted: 24 November 2017 / Published online: 4 December 2017


**Abstract**
Lung tumors are a frequent type of cancer in humans and a leading cause of death, and the late diagnostic contributes to high mortality rates. New therapeutic strategies are needed, and the heptapeptide angiotensin-(1-7) [ang-(1-7)] demonstrated the ability to control cancer growth rates and migration in vitro and in vivo. However, the possible use of the heptapeptide in clinical trials demands deeper analyses to elucidate molecular mechanisms of its effect in the target cells. In this study, we investigated relevant elements that control pro-inflammatory environment and cellular migration, focusing in the post-transcription mechanism using lung tumor cell line. In our cellular model, the microRNA-513a-3p was identified as a novel element targeting ITG-β8, thereby controlling the protein level and its molecular function in the controlling of migration and pro-inflammatory environment. These findings provide useful information for future studies, using miR-513a-3p as an innovative molecular tool to control lung tumor cell migration, which will support more effective clinical treatment of the patients with the widely used chemotherapeutic agents, increasing survival rates.

**Keywords** Cellular migration processes · Pro-inflammatory environment · Small non-coding RNAs · Tumorigeneses · Vasoactive peptide

## Introduction

Over the last few years, lung tumors have emerged as the most frequent type of cancer in humans and a leading cause of death [1]. Basically, there are two main types of lung cancer: the small lung cancer (SLC) and the non-small cell lung cancer (NSCLC), which represents almost 90% of the cases [2]. Considering the late diagnosis of such diseases, high incident of metastases is frequently found in patients, which contributes to low survival rates [3, 4]. However, despite all the improvement in therapeutics to treat cancer in the last decades, a deep understanding of cellular mechanisms that support migration and metastasis is still missing. The elucidation of molecular markers that control such cellular processes will contribute to the improvement of the lung cancer treatment and patients' life expectancy. More recently, the heptapeptide angiotensin-(1-7) [ang-(1-7)] has demonstrated a direct ability to control the growth rates of lung cancer cells in vitro and in vivo [5–8]. The peptide is a product of the renin–angiotensin system (RAS) and was initially described by its effect in the control of the cardiovascular system [9, 10]. This vasoactive peptide plays relevant functions in cellular signaling through the activation of its G-protein-coupled receptor, Mas [11], and a better understanding of the mechanisms and the central elements modulated by the ang-(1-7) in the controlling of tumor migration is a promising strategy for an innovative therapeutic development.

✉ Karen C. M. Moraes
Karenmor@rc.unesp.com

[1] Laboratório de Biologia Molecular, Departamento de Biologia, Instituto de Biociências, Universidade Estadual Paulista "Júlio de Mesquita Filho", Rio Claro, São Paulo 13506-900, Brazil

[2] Instituto de Química, Universidade Estadual Paulista "Júlio de Mesquita Filho", Araraquara, São Paulo, Brazil

[3] Núcleo de Pesquisa em Biologia, Universidade Federal de Ouro Preto, Ouro Preto, Minas Gerais, Brazil

[4] Laboratório de Fisiologia, Departmento de Fisiologia e Biofísica, Universidade Federal de Minas Gerais, Belo Horizonte, Minas Gerais, Brazil

In tumor cells, there are intricate signaling pathways and the inflammatory process is present. Under a pro-inflammatory environment, the arachidonic acid (AA) pathway is activated and induces the expression of cyclooxygenase-2 (COX-2) or prostaglandin-endoperoxide synthase 2 (PTGS2), which plays a major function in the control of this cellular pathway [12]. The mechanisms by which COX-2 controls the inflammatory process have been studied for decades, and in tumors, the pro-inflammatory environment modulates the progression of the disease. In lung cancer, COX-2 overexpression was observed, and, more recently, the cellular activity of COX-2 has been pointed as a relevant element that helps control cellular migration [13, 14]. Moreover, in cancers, significant reduction in tumor growth and angiogenesis was observed when the patients were treated with COX-2 inhibitors (coxib) [15]; however, because of the considerable increased rates of cardiovascular accidents, their use are restricted [16, 17]. On the other hand, the ang-(1-7) is a potential candidate to safe control COX-2 protein levels [15, 18, 19] considering the antithrombotic and anti-inflammatory properties of the peptide that directly benefit the cardiovascular system [20–22]. In system biology, the AA pathway can also be modulated by the pI3K/AKT pathway, which is directly influenced by the effect of the ang-(1-7) [23–25]. The pI3K/AKT pathway modulates cellular apoptosis, inflammation, migration, and glycolysis metabolism, among others, reinforcing the observation of interconnected cellular pathways between inflammatory and migratory processes. In addition, an increasing number of investigations demonstrated that microRNAs (miRNAs) are directly involved in the control of the fine regulation of gene expression in tumor cells. More recently, studies have been pointing the modulatory function of miRNAs in the controlling of COX-2 enzyme [26–29] and cellular migration [7, 8].

MicroRNAs are small non-coding RNAs (21–25 nts) that regulate gene expression by binding to the 3′-untranslated region (UTR) of target mRNAs, which decreases the protein synthesis. It is known that these small molecules act in a synchronized way and the precise description of the molecular networks controlled by miRNAs will contribute to the biotechnological and pharmaceutical innovations. Thus, in the present study we decided to investigate the modulatory effect of the heptapeptide in the pro-inflammatory cellular mechanisms, focusing on the regulatory function of miRNAs to characterize central elements that control cellular migration. Therefore, the analyses revealed an innovative function of the miR513a-3p in controlling levels of the integrin-β8 protein, which is connected to the maintenance of cellular adhesion, disrupted during the metastatic processes.

## Materials and methods

### Cell culture and treatments

A549 lung carcinoma cells (American Type Culture Collection, ATCC®: CCL-185™) were grown and maintained in Dulbecco's Modified Eagle Medium/Nutrient Mixture F-12 (DMEM/F12) supplemented with 4 mM of L-glutamine and 10% of fetal bovine serum (FBS) in a 5% $CO_2$ atmosphere at 37 °C. All reagents were purchased from Thermo Fisher Scientific, USA. For experiments, cells were seeded in 75 $cm^2$ plates at the density of $3.2 \times 10^3$ cells/$cm^2$, and the heptapeptide ang-(1-7) (Merck, Millipore, USA) was added or not to the cultures at a final concentration of $10^{-7}$ M [7]. The culture media were renewed every 24 h until the cultures reached ~90% confluency. For A549 -pEP-miR cellular clones, puromycin (Sigma-Aldrich) was added to the media at the final concentration of 1 µg/ml.

### COX-2 enzyme activity and PGE2 immunoassays

COX-2 activity was measured according to the instructions of the manufacturer of the COX Activity Assay (Cayman Chemical, USA). In doing so, $1.2 \times 10^8$ cells from each independent group were resuspended in 50 µl of cold buffer (0.1 M Tris–HCl, pH 7.8, containing 1 mM ethylenediamine tetraacetic acid, EDTA) and next centrifugated at 4 °C for 15 min. The supernatants were used to measure COX-2 activity which was assessed using the selective COX-1 inhibitor SC-560. For the prostanoid prostaglandin E2 (PGE2) measurement, cell culture supernatants were collected and used in immunoassays. Fifty (50) µl of the cellular supernatants were used in each assay and PGE2 was measured using specific ELISA kit from Cayman Chemical, USA, as directed by the manufacturers. The assays were analyzed with a microplate reader (Packard Instrument Company Inc., USA), and the experiments were performed in triplicate.

### Plasmid constructs and cell line establishment

The cDNA sequences of corresponding regions of precursors miRNAs-513a-3p and -4465 were amplified by conventional polymerase chain reaction (PCR) using appropriate primers set (miR-513a-3p: 5′-TCGAGGATCCAGGCACAAAAAGTTCCTTGAAG and 5′-TCGAGCTAGCGGGATGCCACATTCAGCCATTC; miR-4465: 5′-TCGAGGATCCCTACAAAGGATGTTACAGTTG and 5′-TCGAGCTAGCCAAGTTATATGCTATTGAAAC). The amplified fragments were cloned between *Nhe* I and *Bam* HI cloning sites of miRNASelect™ pEP-mir Expression Vector (Cell Biolabs Inc.) and the plasmids were used to A549 transfection

using Lipofectamine 2000 transfection reagent (Thermo Fisher Scientific, USA) following the instructions of the supplier. The miRNASelect™ pEP-mir Null Control Vector was used as plasmid control in the assays. Cellular clones were selected using 1 µg/ml of puromycin.

## Cellular transfections for small interfering RNA (siRNA)

For small interfering RNA (siRNA) analyses, $5 \times 10^4$ A549 cells were plated on a 24-well plate incubated overnight under regular growth conditions. Next, 20 nM ITG-β8 siRNA or its Non-targeting Pool (On-Target Plus siRNA—Smart Pools—Dharmacon/GE Health Care, USA) were transfected into cells using Lipofectamine 2000 transfection reagent (Thermo Fisher Scientific, USA) as previously described. At 48 h, cells were collected for further investigation.

## RNA isolation and quantitative PCR

Total RNA from ang-(1-7)-treated and untreated A549 cultures or from A549-pEP-miR clones were isolated according to Da Silva et al. [30]. For that $1.0 \times 10^6$ cells were collected and the RNA was extracted using TRIZOL® Reagent (Thermo Fisher Scientific, USA). Two hundred nanograms from each RNA sample were reverse-transcribed (RT) into first-strand cDNA using High-Capacity cDNA Reverse Transcription (Thermo Fisher Scientific, USA) following the suppliers' instructions. Next, the expression levels of the investigated genes was measured by real-time quantitative PCR with the SYBR® Green PCR Master Mix (Applied Biosystems®—ThermoFisher Scientific, USA) on an Applied Biosystems® 7500 Real-Time PCR (Applied Biosystems®, Thermo Fisher Scientific, USA). The reactions were run in triplicate, and mRNA expression was normalized to the reference gene *β-actin*. The specific primers set used at 0.75 µM in these analyses were as follows: *β-actin*, 5′-CGGGACCTGACTGACTAC and 5′-CTCCTTAATGTC ACGCAC; AKT, 5′-GCTTACTGAGAACCGTGTCC and 5′-GGTCGTGGGTCTGGAATG; *COX-2*, 5′-CAGCAC TTCACGCATCAG and 5′-CTAGCCAGAGTTTCACCG ; *FOXO1*, 5′-GCCTGACCCAAGTGAAGAC and 5′-GCC CATTCTGCCATAGCC; *CLDN1*, 5′-CTCCCTGACAAT GTATCC and 5′-ATGAAGAGAGCAGAAGCC ; *EPCAM*, 5′-GGTTGTGGTGATAGCAGTTG and 5′-GCCTTCTCA TACTTTGCC; *Integrin –β8*, 5′-AGATTGCTGCTGGTG ATG and 5′-ACAGTTTCCGTCATTGGG. The results were quantified as $C_t$ values and presented as relative gene expression (the ratio of target/control). The $2^{-\Delta\Delta C_t}$ method was used to calculate the relative quantification.

For miRNA analyses, the 3′-UTR sequence of FOXO1 and COX-2 was extensively analyzed using online bioinformatics tools such as miRBase [31], miRDB [32], and Blast search to identify common miRNAs that could control the post-transcriptional level of those molecules. For the assay, total RNA purified from cell cultures were used in reverse transcription reactions using Mini Script Reverse Transcription reagent (Qiagen®, Germany). The expression levels of hsa-miR-513a-3p and hsa-miR-4465 were performed using real-time quantitative PCR with miScript SYBR Green PCR Kit (Qiagen®, Germany) according to the manufacturer's instructions. The same Applied Biosystems® 7500 Real-Time PCR (Applied Biosystems®, Thermo Fisher Scientific, USA) equipment was used to apply the $2^{-\Delta\Delta C_t}$ analyses to relative quantification method; U6 was adopted as an internal control. The results were quantified as $C_t$ values and used to calculate relative gene expression.

## Wound healing, agarose spot invasion, and Boyden chamber assays

Wound healing assays were performed according to the protocol described in Silva et al. [8]. For that, A549 group of cells and their clones were grown under specific condition in 6-well plates until confluence. Next, a straight-lined wound was made with a sterile 200-µl pipet tip, which created a cell-free wound area by scrapping off the cells. Cells were washed with PBS and fresh culture medium was replaced. Immediately, after the wound (0-h time-point) and after 24 h, cells were photographed under phase-contrast microscopy to measure the migration of the cells into the wound. The assays were performed in triplicate, and mean values of consecutive tracings were used to compute the percentage of closure from the original wound.

Agarose spot assay for cellular invasion was performed as described in Wiggins and Rappoport [33]. Agarose-spots were prepared with DMEN-F12 and 0.5% agarose low melting containing or not 10% FBS (complete culture media) were plated into 6-well plates. Next, $3 \times 10^4$ cells were plated in the presence of complete culture media, containing or not the ang-(1-7). Cells that invaded the agarose spot, after 24 and 48 h of incubation, were photographed and counted using a phase-contrast microscopy (BX51 OLYMPUS). Ten randomly selected fields were analyzed.

Boyden chamber or transwell chamber invasion assays were performed in 24-well Corning BioCoat™ Matrigel® Invasion Chamber plates containing a 8.0-micron-pore size polyester (PET) membrane. For each assay, $2.0 \times 10^4$ cells were suspended in a medium containing 0.4% of serum and seeded into the upper wells. The lower chamber were filled with 850 µl of complete medium and further incubated under regular culture condition (5% $CO_2$ atmosphere at 37 °C) for 24 h. Next, cells that migrated to the lower chamber were fixed and stained with 100% methanol and 1% toluidine blue, respectively, and next analyzed in a phase-contrast

microscopy. Ten randomly selected fields were analyzed per assay and three sets of experiments were performed.

### Western blot analyses

Fifty micrograms of whole cell extracts of A549 and A549-pEP-miR clones, prepared as described previously [30], were separated by electrophoresis in 10% polyacrylamide gels and then electrotransferred to polyvinylidene fluoride (PVDF) membranes. The membranes were immunoblotted overnight at 4 °C with the murine anti-COX-2 (Cayman Chemical, USA), anti-Integrin-β8 (Santa Cruz Biotech, USA), anti-EPCAM, and anti-β actin (Cell Signaling. Inc, USA) polyclonal antibodies, followed by 2-h incubation with a horseradish peroxidase-conjugated goat anti-rabbit antibody (Santa Cruz Biotech). Immunoreactive bands were visualized with a chemiluminescent detection kit (ECL™, GE Healthcare, USA) and exposed to hyperfilm (GE Healthcare, USA). The bands were quantified with the Quantit One® Software (Biorad).

### Dual-luciferase reporter assays

Corresponding cDNA sequence of the 3′-UTR of the Integrin-β8 mRNA (5031–5067 bp, 5′-CCUACAGAUAAA UGUGAAAUUU) or was cloned into the pGL3-Control vector (Promega) upstream of the firefly luciferase coding sequence via synthetic oligonucleotides ligation. In this assay, A549 cells were plated at a density of $6 \times 10^4$ cells per well in a 24-well plate and transiently transfected with 100 ng of the pGL3-Control vector or 100 ng of pGL3-Integrin-β8-3′-UTR or 100 ng of the pGL3-Integrin-β8mut-3′-UTR. In addition, 30 nM of mirVana™miRNA hsa-miR-513-a-3p mimic or inhibitor (ThermoFisher Scientific, USA) was also used in the transfection reactions processed with the Lipofectamine® 2000 transfection reagent (ThermoFisher Scientific, USA). The Renilla luciferase reporter plasmid (pRL-TK) was used as the internal control for the transfection efficiency, and at 24 h post transfection, the activities of luciferase were determined using the Promega dual-luciferase reporter assay (Promega, USA) according to the manufacturer's instructions. The *Renilla* luciferase activity was normalized in each sample to account for differences in transfection efficiency. The luciferase activities were measured using a TD20/20 luminometer (Turner Designs).

### Graphs and statistical analyses

Values from at least three independent assays were used for analysis, and graphs were generated using Graph Pad Prism® 5. Data are presented as the mean ± standard deviation and the differences between the control and treated groups as well as the A549-pEP-miR Null and the A549-pEP-miR cell clones were measured using one-way analysis of variance (ANOVA), followed by Dunnett's test. Significance was set at $*p < 0.05$, $**p < 0.01$, and $***p < 0.001$.

## Results

### Ang (1-7) modulates the pro-inflammatory environment: the fine-tuning that controls A549 cell migration

To explore the effect of the ang-(1-7) in lung tumor cells, A549 cells were used as our model of study. Figure 1a presents a schematic illustration of the pI3K/AKT pathway and its connectors.

Then, to explore elements that control cellular migration and inflammation in a close connection mechanism, we investigated mRNA expression levels of AKT, COX-2, and FOXO1 in our cellular model. The results presented in Fig. 1b demonstrated significant increase in FOXO1 level (~ 44%), reinforcing the observations that ang-(1-7) modulates FOXO1 activity [19, 34]. This protein is characterized as a transcription factor that belongs to the forkhead family and the molecule controls different cellular mechanisms such as cell cycle, proliferation, differentiation, and even cellular metastasis [25].

To determine post-transcriptional regulatory elements that modulate FOXO1 in the pro-inflammatory environment, bioinformatics analyses identified common putative binding sites in the 3′-UTR sequences of COX-2 and FOXO1 mRNAs for the miRNA 513a-3p and -4465. The analyses are illustrated by a Venn's diagram (Fig. 1c). Next, the expression levels of the miRNA 513a-3p and -4465 were determined in A549 heptapeptide-treated and -untreated cells. The results point a significative effect of the ang-(1-7) in the expression levels of the investigated miRNAs (~ 100% increase in the miRNA expression level). To address how those miRNAs modulates cellular migration under tumoral pro-inflammatory cellular environment, permanent clones overexpressing the miRs-513a-3p or -4465 were established and the miRNA expression level found in those cells was similar to what was found in A549 heptapeptide-treated cells (Fig. 1d). The clone containing the pEP-miR Null Control was used as experimental control of the assays. Moreover, COX-2 protein level and activity and PGE2 were measured for all the investigated groups. In heptapeptide and in pEP-miR-513a-3p clone, the investigated elements reduced similarly (Fig. 1e).

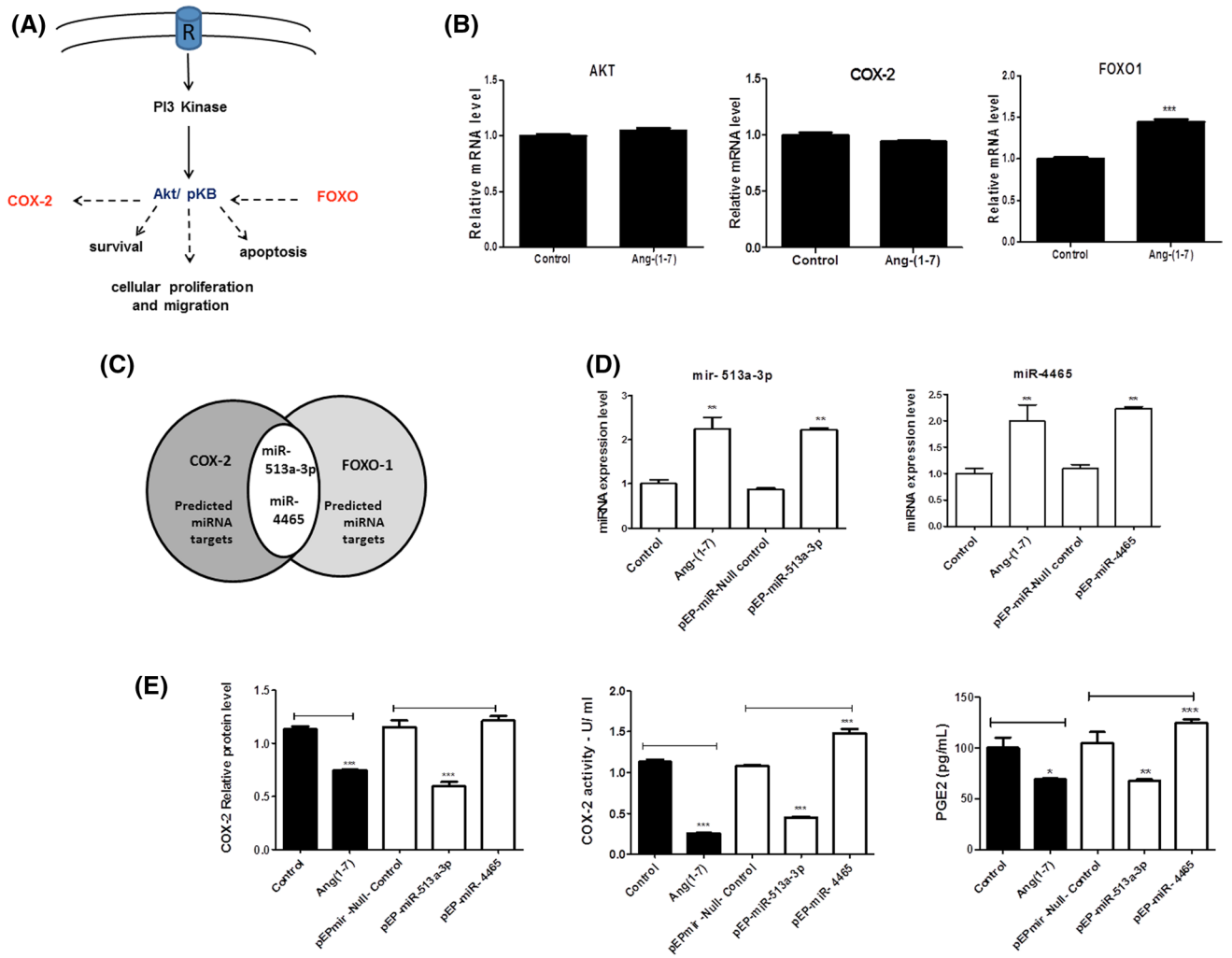


**Fig. 1** Angiotensin-(1-7) modulates the pro-inflammatory environment in tumor cells through the activation of AKT/pKB signaling pathway. **a** Schematic representation of molecular connections mediated by the AKT/pKB cellular signaling. In the figure, it is also represented the modulatory effect of FOXO1 on COX-2 activity through the AKT activity. **b** AKT, COX-2, and FOXO1 mRNA expression levels in A549 treated or untreated with the heptapeptide. **c** Venn diagram illustrating the potential microRNAs that co-regulate COX-2 and FOXO1 mRNAs. **d** Expression patterns of miRNA-513a-3p and miRNA-4465 that putatively bind to the 3′-UTR sequence of the COX-2 and FOXO1 mRNAs in ang-(1-7)-treated and -untreated cells. **e** COX-2 relative protein level, COX-2 activity, and PEG2 measurement in all investigated cellular groups. Values are mean ± SE from at least three independent experiments; the significance level was set at $^{***}p < 0.05$

## Modulatory effect of the angiotensin-(1-7) and the miRs-513a-3p and -4465 in A549 cell migration

To address the physiologic effect of either the heptapeptide or the investigated miRNAs in A549 migration, wound healing assays were performed. Figure 2a presents the results. In control cultures, 88.6% recovery of injured area was observed after 24 h of culture scratch. Similar recovery percentage was observed in A549-pEP-miR Null Control and A549-pEP-miR-4465 clones. In the heptapeptide-treated cultures, 58.6% recovery was observed and in the A549-pEP-miR-513a-3p cells 43.7% recovery of the wound was verified. Next, to evaluate cell motility, the agarose spot assay was performed (Fig. 2b). Time lapses demonstrated the migration of the cells into the agarose spots in different A549 cellular groups. Pronounced increased rates of cell migration were observed for the A549-pEP-miR-4465; on the other hand, the A549-pEP-miR-513a-3p presented lower migration rate into the agarose spot. The same results were observed in transwell chamber invasion assays performed for all the investigated groups of cells (Fig. 2c).

Considering the results, extensive search in miRBase [31] and miRDB [32] algorithms were conducted to identify potential common target molecules for the investigated miRNAs that could possibly control cellular migration rate.

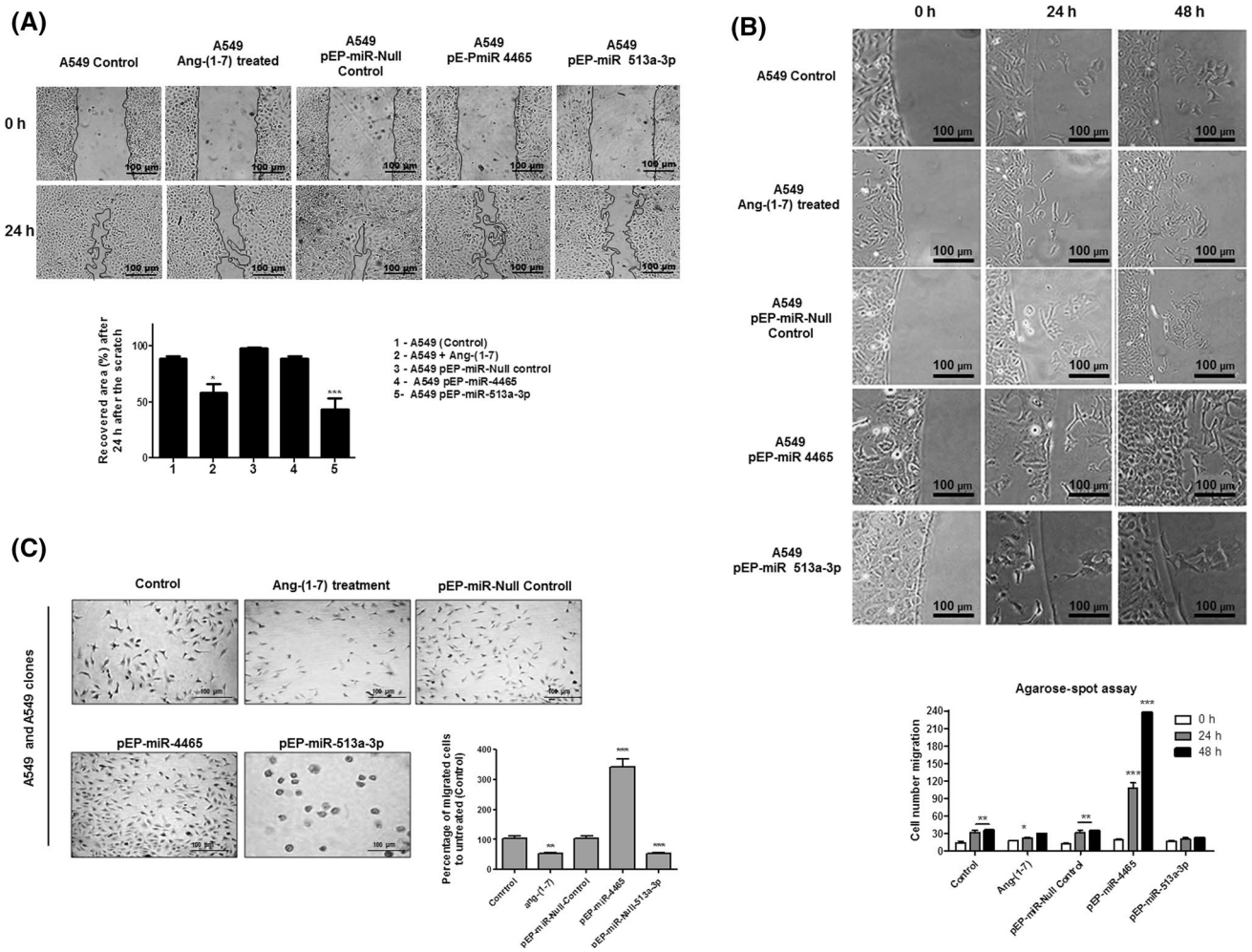


**Fig. 2** Effect of ang-(1-7) and the overexpression of miR-513a-3p and miR-4465 in A549 migration rate. **a** Cell migration was analyzed immediately after the scratch (0 h) and at 24-h time-point. The black lines delineated the margin of the gaps. **b** Bovine serum directed chemotaxis in different groups of A549 lung tumor cells in agarose spot assay. Cellular migration was verified and quantified and the results were plotted in a graph. **c** Transwell chamber invasion assays of A549 and A549 clones. Representative results are presented. Values are mean ± SE from at least three independent experiments; the significance level was set at $***p < 0.05$

Three molecules were selected to be analyzed: claudin 1(CLDN1) is an integral membrane protein and component of tight junctions that is strict correlated to the cell–cell adhesion; epithelial cell adhesion molecule (EPCAM) is a calcium-independent cell adhesion molecule; and, integrin subunit beta 8 (ITG-β8), which plays relevant function in cell–cell and cell–extracellular matrix interaction. The mRNA expression level presented in Fig. 3a demonstrated no major changes in CLDN1 expression between the cellular groups. On the other hand, the analyses pointed increased expression level of EPCAM mRNA in A549-pEP-miR-4465 (2.7 x higher than the control group) and reduced level of ITG-β8 mRNA in the A549-pEP-miR-513a-3p clone, nearly comparable to the level found in A549 heptapeptide-treated cells. Based on the qPCR results, Western blot quantification was performed for the EPCAM and ITG-β8 proteins (Fig. 3b), which presented similar expression patterns to the mRNA level.

To determine if ITG-β8 3′UTR is a true target of miR-513a-3p, dual-luciferase assays were performed (Fig. 4a). The ITG-β8-3′-UTR construct decreased the luciferase production by ~ 16% in transfected cells compared to the cells transfected with the pGL3-Control vector. Moreover, the transfection of A549 with miRNA 513a-3p mimics decreased the luciferase production by 48%, suggesting that this miRNA blocks the luciferase production mediated by the RNA interference (RNAi) mechanism. On the other hand, the miRNA 513a-3p inhibitor increased the luciferase production by 16.4% compared to the control group, suggesting that this molecule blocks the natural miRNA binding to the 3′-UTR of ITG-β8, facilitating extra rounds of ITG-β8 translation.

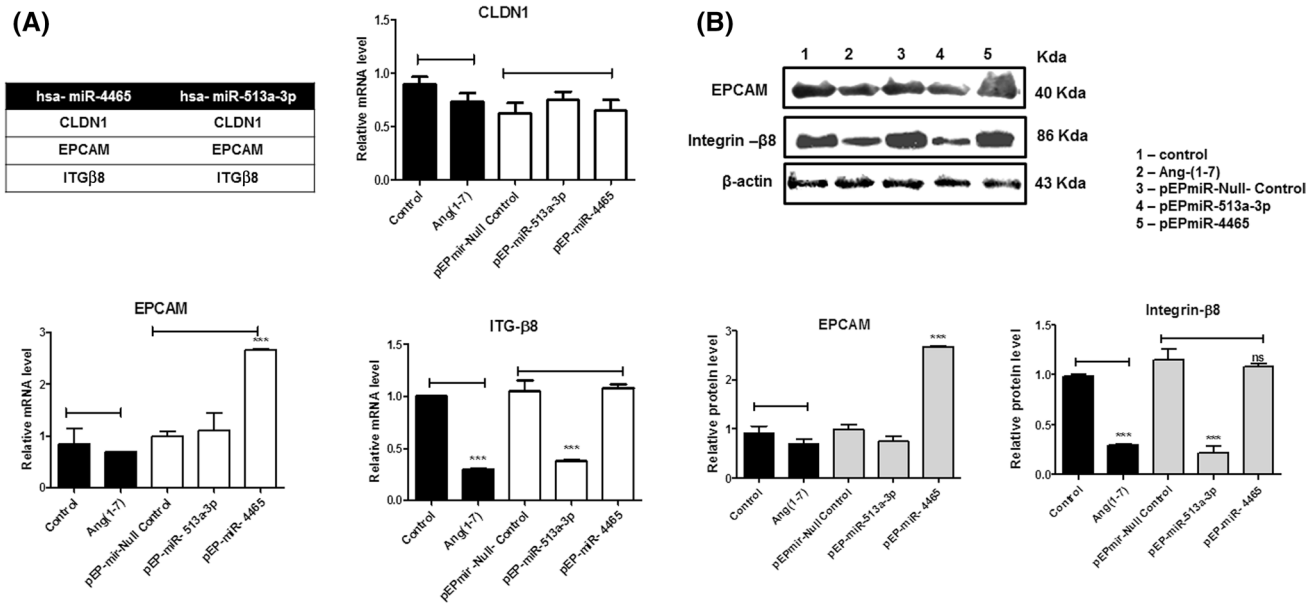


**Fig. 3** Transcriptional and post-transcriptional levels of potential target molecules of the miR-513a-3p and miR-4465. **a** CLDN1, EPCAM, and ITG-β8 mRNA levels in different groups of A549. **b** Western blot analyses of EPCAM and ITG-β8 proteins in A549 cells. Values are mean ± SE from at least three independent experiments; the significance level was set at $***p < 0.05$

Next, functional validation of the ITG-β8 was performed. Figure 4b demonstrates that 20 nM ITG-β8 siRNA reduced the ITG-β8 protein level in 88% in A549, when compared to the protein level found in activated and non-transfected cells. In addition, the effect of siITG-β8 was evaluated in wound healing (Fig. 4c), agarose spot assays (Fig. 4d), and through transwell chamber invasion assays (Fig. 4d), which demonstrated reduced migration rates when compared to the unmodified A549 cells (Fig. 2). Otherwise, cells transfected with the Non-targeting Pool of ITG-β8 siRNA (Scramble siRNA) did not change the protein level of ITG-β8 nor the migration rates in wound healing or agarose spot assay (data not shown).

## Discussion

In this study, the A549 lung tumor cell line was used to address elements modulated by the heptapeptide ang-(1-7) that could contribute to the control of cellular migration under an anti-inflammatory environment. It is known that the angiotensin-(1-7) is a peptide hormone that modulates pI3K/AKT activity in the controlling of inflammation and cellular migration [24, 25]; however, the identification of central elements that coordinates those cellular processes is still unknown.

In the literature, despite the fact that no significative direct interaction between FOXO1 and the COX-2 protein was demonstrated, it was described that AKT plays a major function as cellular connector between those proteins [19, 35]. Then, the mRNA levels of those molecules were verified and despite no COX-2 mRNA levels change were verified, the modulatory activity of the peptide decreased COX-2 protein level and activity, as well as the PGE2 production (Fig. 1). This observation reinforced previous results found in other studies [6, 36]. The same observation for COX-2 metabolites was verified in the clone miR-513a-3p. In addition, the decreased COX-2 protein level in our assays is probably connected to post-transcriptional controlling mechanisms, which blocks translational processes through the RNAi [37]. In system biology, this modulatory activity of the miR-513a-3p helps control the pro-inflammatory environment in tumoral cells.

Moreover, the results observed in wound healing, agarose spot, and transwell chamber invasion assays for the pEP-miR-513a-3p cell clone reinforced the relevant cellular physiological function of this miRNA in controlling the migration rate of A549 cells based on what was observed in ang-(1-7)-treated cells (Fig. 2). Opposite results were observed for the activity of miR-4465 in all the investigated aspects.

To better explore molecular connections that support the modulatory function of the miR-513a-3p in A549 migration, bioinformatics approaches were addressed to identify potential elements that could be modulated by either the miR-513a-3p or miR-4465. Three different proteins that influence cellular migration were pointed. Based on the mRNA expression patterns observed in the assays,

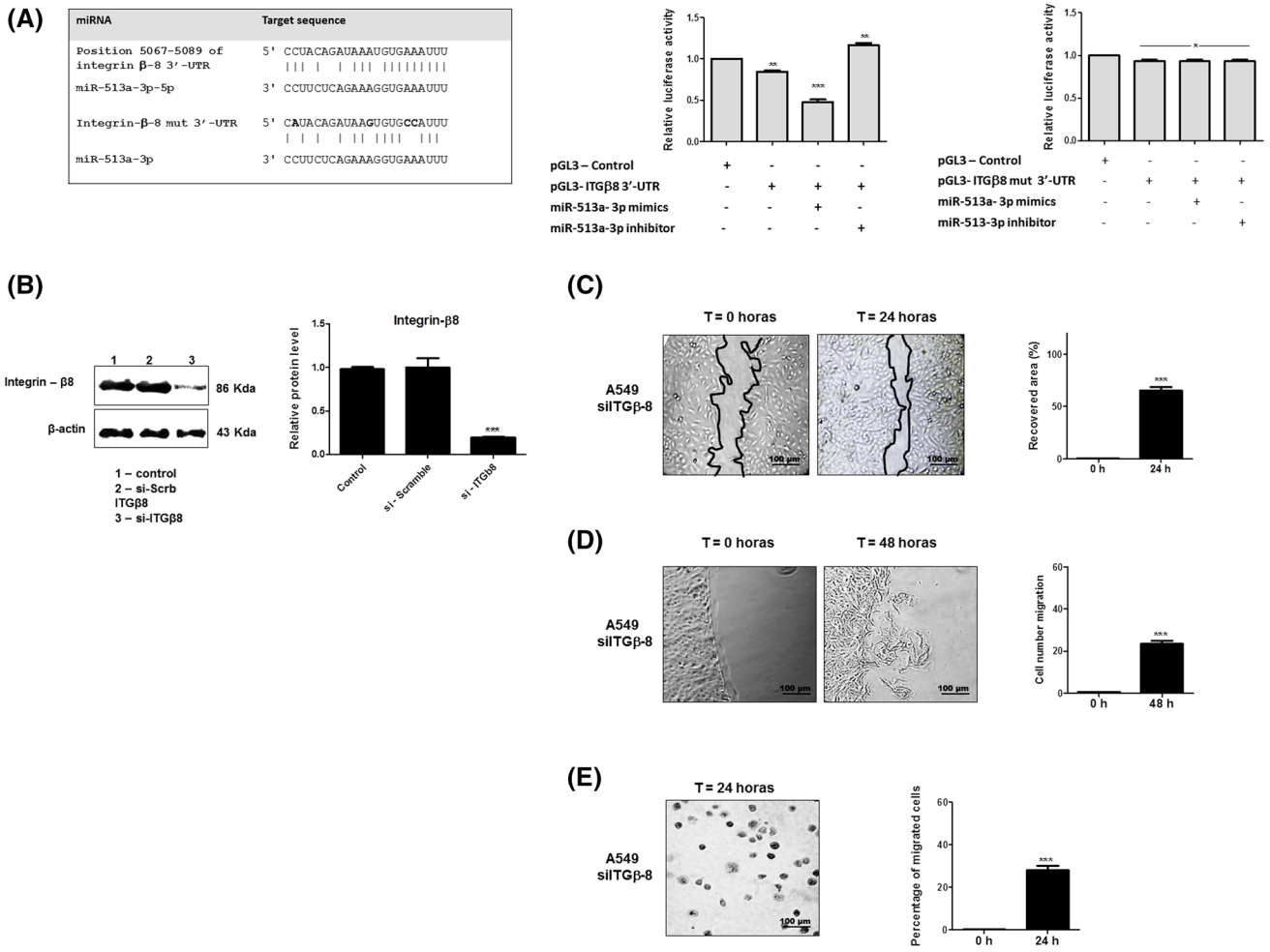


**Fig. 4** Functional mechanisms of ITG-β8 as a direct target of miR-513a-3p. **a** Schematic sequence cloned in pGL3 plasmids, and the relative luciferase activity in cells co-transfected with them (pGL3 plasmids Control, ITG-β8-3′-UTR or ITG-β8mut 3′-UTR) and the miRNA-513a-3p or the miRNA-513a-3p inhibitor; the results were plotted in representative graphs. **b** The effect of ITG-β8 gene silencing was evaluated in groups of A549 by Western blot analyses. β-actin was used as the loading control. **c** Cell migration was analyzed in siITG-β8-A549 cells immediately after the scratch (0 h) and at 24-h time-point. The black lines delineated the margin of the gaps. **d** Serum bovine-directed chemotaxis in siITG-β8-A549 cells in agarose spot assay. **e** Transwell chamber invasion assays of siITG-β8-A549 cells. Cellular migration, chemotaxis, and invasion assays were verified and quantified and the results were plotted in graphs. Values are mean ± SE from at least three independent experiments; the significance level was set at $^{***}p < 0.05$

the proteins EPCAM and ITG-β8 were chosen to be investigated. EPCAM, whose expression is frequently increased in tumors [38, 39], presented high expression level in A549-miR-4465 clones, which supports their increased rates of cellular migration [40–42] (Fig. 3). Moreover, the ITG-β8 demonstrated a downregulated expression pattern in ang-(1-7)-treated cells as well in miR-513a-3p-clones. The ITG-β8 was demonstrated to be connected to cellular proliferation and migration [43, 44] and in our assays we validated the effect of this protein in A549 migration rates by knocking down the ITG-β8, which reduced the migrations rates as observed in the wound healing, agarose spot, and transwell chamber invasion assays (Fig. 4).

As a conclusion, in this study, we demonstrated a novel modulatory effect of the heptapeptide ang-(1-7) in controlling cellular migration processes through the functional activity of the miR-513a-3p. The miR-513a-3p binding activity to the ITGβ-8 mRNA activates RNAi, reducing the protein level, which plays relevant function in A549 cellular migration. Previous studies pointed a close connection between pro-inflammatory environment and the expression of ITGβ-8 [45, 46], which act as a positive feedback loop in cellular metastasis. In our assays, the peptide and the miR-513a-3p also demonstrated negative modulatory effect in cellular migration and in the pro-inflammatory environment, which is relevant to the control of the cancer metastasis. In

addition, miRDB and Targetscan [47] algorithms point relevant molecules as potential targets for the interaction of the miR-513a-3p that also connects to the controlling of the pro-inflammatory environment (prostaglandin receptors F, EP2, EP3, EP4, etc, and microsomal glutathione S-transferase, MGST1), reinforcing the systemic relevance of the investigated miRNA in this cellular metabolic processes. Other elements connected to the cellular architecture and migration, such as activated leukocyte cell adhesion molecule (ALCAM), protocadherin-related 15 (PCDH15), PCDH8, PCDH 17, etc., were also pointed as potential target molecules of the mir-513a-3p. Moreover, the miR-513a-3p helps sensitize human lung adenocarcinoma cells to chemotherapy by targeting Glutathione S-transferase P1 (GSTP1) [48], a molecule that contributes to cisplatin resistance, reinforcing the relevance of the miR-513a-3p in controlling cancer metastases.

Future in vivo investigations will help elucidate the fine-tuning of the cancer metastasis controlling and the modulatory effect of the miR-513a-3p in system biology. Besides, the development of innovative therapeutic approaches that increase the miRNA 513a-3p level in injured tissue may contribute to the reduction of metastatic rates, which will support more effective clinical treatment of the patients with the widely used chemotherapeutic agents, increasing survival rates.

**Acknowledgements** This study was supported by research grants from the Conselho Nacional de Desenvolvimento Científico e Tecnológico (CNPq) (474060/2012-8), Fundação de Amparo à Pesquisa do Estado de São Paulo (FAPESP—2014/21645-2; 2013/21186-5), and INCT-Nano-Biofarmacêutica. The authors report no conflict of interest.

## References

1. World Health Organization (2015) Fact sheet no. 297. WHO Press. http://www.who.int/mediacentre/factsheets/fs297/en/
2. Nascimento AV, Bousbaa H, Ferreira D, Sarmento B (2015) Non-small cell lung carcinoma: an overview on targeted therapy. Curr Drug Targets 16:1448–1463. https://doi.org/10.2174/1389450115666140528151649
3. Ellis PM, Vandermeer R (2011) Delays in the diagnosis of lung cancer. J Thorac Dis 3:183–188. https://doi.org/10.3978/j.issn.2072-1439.2011.01.01
4. Gildea TR, DaCosta Byfield S, Hogarth DK, Wilson DS, Quinn CC (2017) A retrospective analysis of delays in the diagnosis of lung cancer and associated costs. Clinicoecon Outcomes Res 9:261–269. https://doi.org/10.2147/CEOR.S132259
5. Gallagher PE, Tallant EA (2004) Inhibition of human lung cancer cell growth by angiotensin-(1-7). Carcinogenesis 25:2045–2052. https://doi.org/10.1093/carcin/bgh236
6. Menon J, Soto-Pantoja DR, Callahan MF, Cline JM, Ferrario CM, Tallant EA, Gallagher PE (2007) Angiotensin-(1-7) inhibits growth of human lung adenocarcinoma xenografts in nude mice through a reduction in cyclooxygenase-2. Cancer Res 67:2809–2815. https://doi.org/10.1158/0008-5472.CAN-06-3614
7. Soto-Pantoja DR, Menon J, Gallagher PE, Tallant EA (2009) Angiotensin-(1-7) inhibits tumor angiogenesis in human lung cancer xenografts with a reduction in vascular endothelial growth factor. Mol Cancer Ther 8:1676–1683. https://doi.org/10.1158/1535-7163.MCT-09-0161
8. Silva Bde O, Lima KF, Gonçalves LR, Silveira MB, Moraes KC (2016) MicroRNA profiling of the effect of the heptapeptide angiotensin-(1-7) in A549 lung tumor cells reveals a role for miRNA149-3p in cellular migration processes. PLoS ONE 11:e0162094. https://doi.org/10.1371/journal.pone.0162094
9. Ferreira AJ, Santos RAS, Almeida AP (2001) Angiotensin-(1-7): cardioprotective effect in myocardial ischemia/reperfusion. Hypertension 38:665–668. https://doi.org/10.1161/01.HYP.38.3.665
10. Loot AE, Roks AJ, Henning RH, Tio RA, Suurmeijer AJH, Boomsma F, van Glist WH (2002) Angiotensin-(1-7) attenuates the development of heart failure after myocardial infarction in rats. Circulation 105:1548–1550. https://doi.org/10.1161/01.CIR.0000013847.0035.B9
11. Santos RA, Simoes e Silva AC, Maric C, Silva DM, Machado RP, de Buhr I, Heringer-Walther S, Pinheiro SV, Lopes MT, Bader M, Mendes EP, Lemos VS, Campagnole-Santos MJ, Schultheiss HP, Speth R, Walter T (2003) Angiotensin-(1-7) is an endogenous ligand for the G protein-coupled receptor Mas. Proc Natl Acad Sci USA 100:8258–8263. https://doi.org/10.1073/pnas.1432869100
12. Curtis-Prior P (2004) The eicosanoids. Wiley Ed, West Sussex
13. Gallagher PE, Cook K, Soto-Pantoja D, Menon J, Tallant EA (2011) Angiotensin peptides and lung cancer. Curr Cancer Drug Targets 11:394–404
14. Li W, Sun D, Lv Z, Wei Y, Zheng L, Zeng T, Zhao J (2017) Insulin-like growth factor binding protein-4 inhibits cell growth, migration and invasion, and downregulates COX-2 expression in A549 lung cancer cells. Cell Biol Int 4:384–391. https://doi.org/10.1002/cbin.10732
15. Kalaitzidis RG, Elisaf MS (2017) Uncontrolled hypertension and oncology: clinical Tips. Curr Vasc Pharmacol. https://doi.org/10.2174/1570161115666170414121436
16. Katz JA (2013) COX-2 inhibition: what we learned—a controversial update on safety data. Pain Med Suppl 1:S29–S34. https://doi.org/10.1111/pme.12252
17. McIntyre WF, Evans G (2014) The Vioxx® legacy: enduring lessons from the not so distant past. Cardiol J 21:203–205. https://doi.org/10.5603/CJ.2014.0029
18. Muthalif MM, Benter IF, Uddin MR, Harper JL, Malik KU (1998) Signal transduction mechanisms involved in angiotensin-(1-7)-stimulated arachidonic acid release and prostanoid synthesis in rabbit aortic smooth muscle cells. J Pharmacol Exp Ther 284:388–398
19. Passos-Silva DG, Verano-Braga T, Santos RA (2013) Angiotensin-(1-7): beyond the cardio-renal actions. Clin Sci (Lond) 124:443–456. https://doi.org/10.1042/CS20120461
20. Patel VB, Bodiga S, Fan D, Das SK, Wang Z, Wang W, Basu R, Zhong J, Kassiri Z, Oudit GY (2012) Cardioprotective effects mediated by angiotensin II type 1 receptor blockade and enhancing angiotensin 1-7 in experimental heart failure in angiotensin-converting enzyme 2-null mice. Hypertension 59:1195–1203. https://doi.org/10.1161/HYPERTENSIONAHA.112.191650
21. Papinska AM, Mordwinkin NM, Meeks CJ, Jadhav SS, Rodgers KE (2015) Angiotensin-(1-7) administration benefits cardiac, renal and progenitor cell function in *db/db* mice. Br J Pharmacol. 172:4443–4445. https://doi.org/10.1111/bph.13225
22. Galandrin S, Denis C, Boularan C, Marie J, M'Kadmi C, Pilette C, Dubroca C, Nicaise Y, Seguelas MH, N'Guyen D, Banères JL, Pathak A, Sénard JM, Galés C (2016) Cardioprotective angiotensin-(1-7) peptide acts as a natural-biased ligand at the angiotensin II type 1 receptor. Hypertension 68:1365–1374

23. Muñoz MC, Giani JF, Dominici FP (2010) Angiotensin-(1-7) stimulates the phosphorylation of Akt in rat extracardiac tissues in vivo via receptor Mas. Regul Pept 161:1–7. https://doi.org/10.1016/j.regpep.2010.02.001
24. Ni L, Feng Y, Wan H, Ma Q, Fan L, Qian Y, Li Q, Xiang Y, Gao B (2012) Angiotensin-(1-7) inhibits the migration and invasion of A549 human lung adenocarcinoma cells through inactivation of the PI3K/Akt and MAPK signaling pathways. Oncol Rep 27:783–790. https://doi.org/10.3892/or.2011.1554
25. Zhang F, Ren X, Zhao M, Zhou B, Han Y (2016) Angiotensin-(1-7) abrogates angiotensin II-induced proliferation, migration and inflammation in VSMCs through inactivation of ROS-mediated PI3K/Akt and MAPK/ERK signaling pathways. Sci Rep 6:34621. https://doi.org/10.1038/srep34621
26. Tanaka T, Haneda S, Imakawa K, Sakai S, Nagaoka K (2009) A microRNA, miR-101a, controls mammary gland development by regulating cyclooxygenase-2 expression. Differentiation 77:181–187. https://doi.org/10.1016/j.diff.2008.10.001
27. Bao B, Ali S, Kong D, Sarkar SH, Wang Z, Banerjee S, Aboukameel A, Padhye S, Philip PA, Sarkar FH (2011) Anti-tumor activity of a novel compound-CDF is mediated by regulating miR-21, miR-200, and PTEN in pancreatic cancer. PLoS ONE 6:e17850. https://doi.org/10.1371/journal.pone.0017850
28. Pham H, Rodriguez CE, Donald GW, Hertzer KM, Jung XS, Chang HH, Moro A, Reber HA, Hines OJ, Eibl G (2013) miR-143 decreases COX-2 mRNA stability and expression in pancreatic cancer cells. Biochem Biophys Res Commun 439:6–11. https://doi.org/10.1016/j.bbrc.2013.08.042
29. Wu K, Yang L, Li C, Zhu CH, Wang X, Yao Y, Jia YJ (2014) MicroRNA-146a enhances Helicobacter pylori induced cell apoptosis in human gastric cancer epithelial cells. Asian Pac J Cancer Prev 15:5583–5586
30. Da Silva W, Dos Santos RA, Moraes KC (2016) Mir-351–5p contributes to the establishment of a proinflammatory environment in the H9c2 cell line by repressing PTEN expression. Mol Cell Biochem 411:363–371. https://doi.org/10.1007/s11010-015-2598-5
31. Griffiths-Jones S, Saini HK, van Dongen S, Enright AJ (2008) miRBase: tools for microRNA genomics. Nucleic Acids Res 36:D154–D158. https://doi.org/10.1093/nar/gkm952
32. Wong N, Wang X (2015) miRDB: an online resource for microRNA target prediction and functional annotations. Nucleic Acids Res 43:D146–D152
33. Wiggins H, Rappoport J (2010) An agarose spot assay for chemotactic invasion. Biotechniques 48:120–123. https://doi.org/10.2144/000113353
34. Verano-Braga T, Schwämmle V, Sylvester M, Passos-Silva DG, Peluso AA, Etelvino GM, Santos RA, Roepstorff P (2012) Time-resolved quantitative phosphoproteomics: new insights into angiotensin-(1-7) signaling networks in human endothelial cells. J Proteome Res 11:3370–3381. https://doi.org/10.1021/pr3001755
35. Uddin S, Ahmed M, Hussain A, Assad L, Al-Dayel F, Bavi P, Al-Kuraya KS, Munkarah A (2010) Cyclooxygenase-2 inhibition inhibits PI3K/AKT kinase activity in epithelial ovarian cancer. Int J Cancer 126:382–394. https://doi.org/10.1002/ijc.24757
36. McCollum LT, Gallagher PE, Tallant EA (2012) Angiotensin-(1-7) abrogates mitogen-stimulated proliferation of cardiac fibroblasts. Peptides 34:380–388. https://doi.org/10.1016/j.peptides.2012.01.020
37. Carthew RW, Sontheimer EJ (2009) Origins and mechanisms of miRNAs and siRNAs. Cell 20:642–655. https://doi.org/10.1016/j.cell.2009.01.035
38. Cimino A, Halushka M, Illei P, Wu X, Sukumar S, Argani P (2010) Epithelial cell adhesion molecule (EpCAM) is overexpressed in breast cancer metastases. Breast Cancer Res Treat 123:701–708. https://doi.org/10.1007/s10549-009-0671-z
39. Endaya B, Guan SP, Newman JP, Huynh H, Sia KC, Chong ST, Kok CYL, Chung AYF, Liu BB, Hui KM, Lam PYP (2017) Human mesenchymal stem cells preferentially migrate toward highly oncogenic human hepatocellular carcinoma cells with activated EpCAM signaling. Oncotarget. https://doi.org/10.18632/oncotarget.17633
40. Gaiser MR, Lämmermann T, Feng X, Igyarto BZ, Kaplan DH, Tessarollo L, Germain RN, Udey MC (2012) Cancer-associated epithelial cell adhesion molecule (EpCAM; CD326) enables epidermal Langerhans cell motility and migration in vivo. Proc Natl Acad Sci USA 109:E889–E897. https://doi.org/10.1073/pnas.1117674109
41. Patriarca C, Macchi RM, Marschner AK, Mellstedt H (2012) Epithelial cell adhesion molecule expression (CD326) in cancer: a short review. Cancer Treat Rev 38:68–75. https://doi.org/10.1016/j.ctrv.2011.04.002
42. Ni J, Cozzi P, Hao J, Beretov J, Chang L, Duan W, Shigdar S, Delprado W, Graham P, Bucci J, Kearsley J, Li Y (2013) Epithelial cell adhesion molecule (EpCAM) is associated with prostate cancer metastasis and chemo/radioresistance via the PI3K/Akt/mTOR signaling pathway. Int J Biochem Cell Biol 45:2736–2748. https://doi.org/10.1016/j.biocel.2013.09.008
43. Xu Z, Wu R (2012) Alteration in metastasis potential and gene expression in human lung cancer cell lines by ITGB8 silencing. Anat Rec (Hoboken). 295:1446–1454. https://doi.org/10.1002/ar.22521
44. Mertens-Walker I, Fernandini BC, Maharaj MS, Rockstroh A, Nelson CC, Herington AC, Stephenson SA (2015) The tumour-promoting receptor tyrosine kinase, EphB4, regulates expression of integrin-β8 in prostate cancer cells. BMC Cancer 15:164. https://doi.org/10.1186/s12885-015-1164-6
45. Worthington JJ, Kelly A, Smedley C, Bauché D, Campbell S, Marie JC, Travis MA (2015) Integrin αvβ8-mediated TGF-β activation by effector regulatory T cells is essential from suppression of T-cell-mediated inflammation. Immunity 42:903–915. https://doi.org/10.1016/j.immuni.2015.04.012
46. Del Rey MJ, Izquierdo E, Usategui A, Gonzalo E, Blanco FJ, Acquadro F, Pablos JL (2010) The transcriptional response of normal and rheumatoid arthritis synovial fibroblasts to hypoxia. Arthritis Rheum 62:3584–3594. https://doi.org/10.1002/art.27750
47. Agarwal V, Bell GW, Nam JW, Bartel DP (2015) Predicting effective microRNA target sites in mammalian mRNAs. Elife. https://doi.org/10.7554/eLife.05005
48. Zhang X, Zhu J, Xing R, Tie Y, Fu H, Zheng X, Yu B (2012) miR-513a-3p sensitizes human lung adenocarcinoma cells to chemotherapy by targeting GSTP1. Lung Cancer 77:488–494. https://doi.org/10.1016/j.lungcan.2012.05.107